

**Cell Reports, Volume 44**

**Supplemental information**

**A cortico-subcortical loop for motor control  
via the pontine reticular formation**

**Emília Bósz, Viktor M. Plattner, László Biró, Kata Kóta, Marco A. Diana, and László  
Acsády**

## Supplemental figures and legends

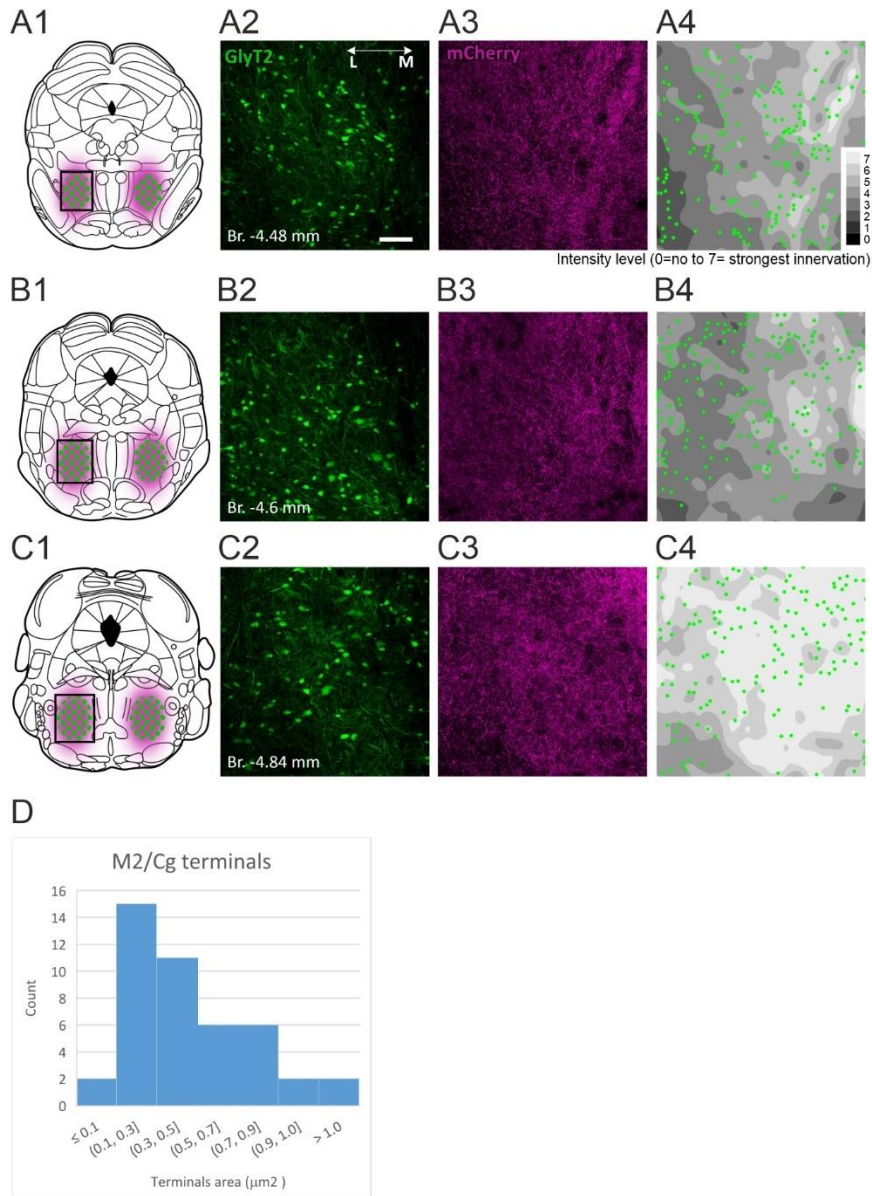


**Figure S1. Fiber density heat maps and cortical terminal size in the PRF. Related to Figure 1.**

A1) Schematic view of the M2/Cg L5 fibers (shady magenta area) around the PRF/GlyT2+ cells (green dots). The black rectangle indicates the position of the micrographs and heatmaps in A2-4.

A2-3) Confocal micrographs of the PRF/GlyT2+ cells (A2) and anterogradely labeled M2/Cg cortical fibers (A3) in a representative animal.

A4) Fiber density heat map (grey shading) and PRF/GlyT2+ neurons (green dots) of the same region. Higher fiber density is indicated with light grey colors.

B-C) As in A) at two more caudal levels. Scale bar: 20  $\mu$ m.

D) Size Distribution of M2/Cg Terminals: the majority of M2/Cg-PRF terminals are classified as either small or medium-sized.

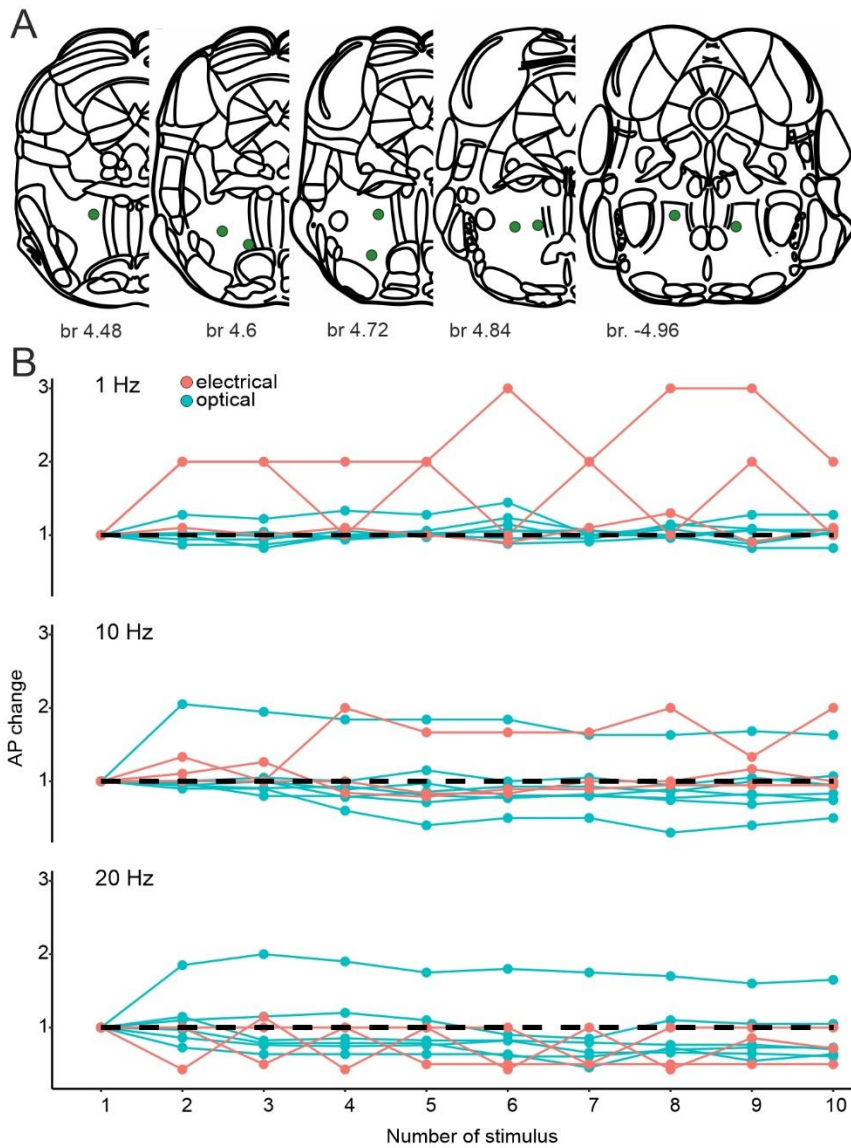
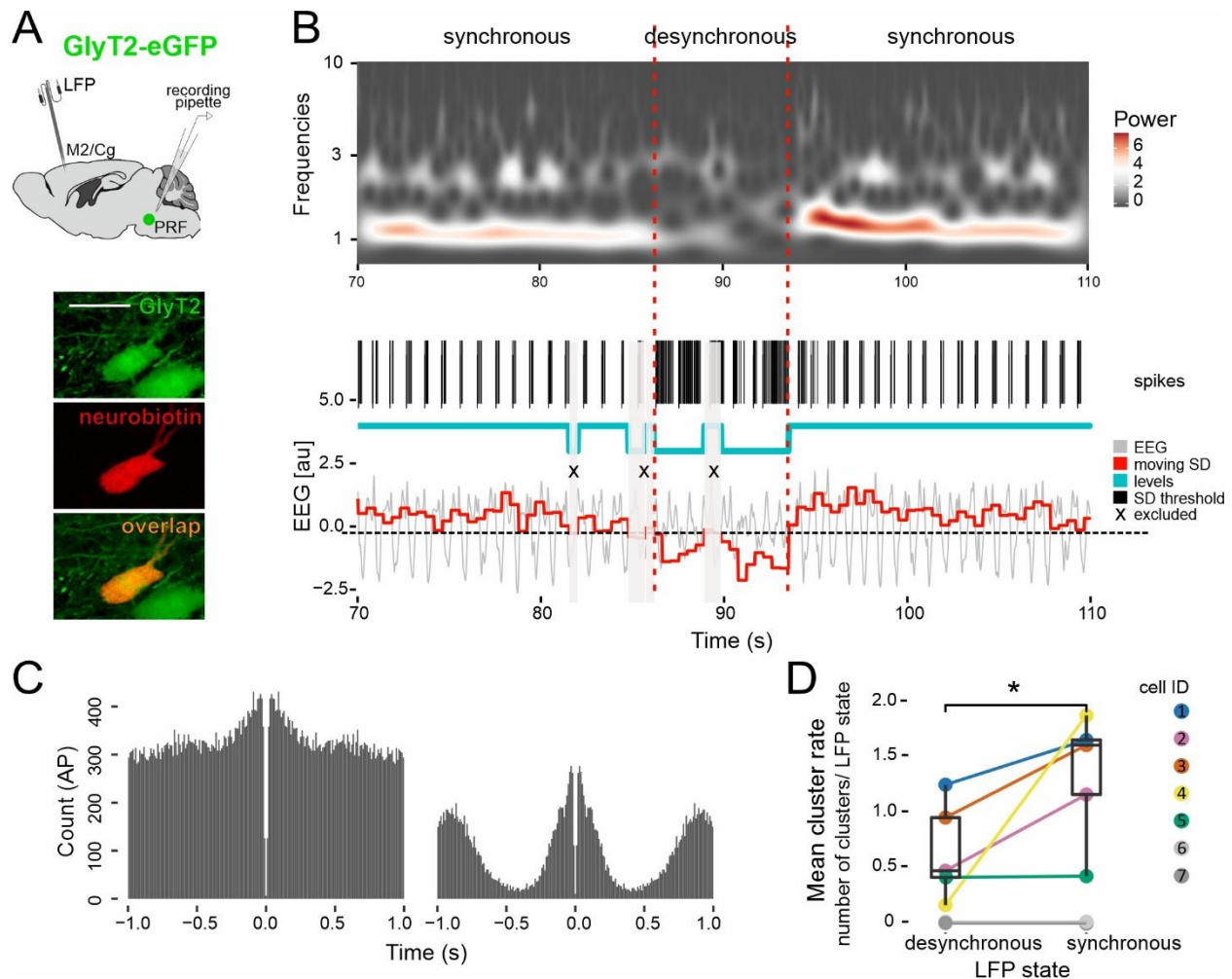


Figure S2. Location of the PRF/GlyT2+ neurons recorded after M2/Cg stimulation and their activity during a stimulus train. Related to Figure 3.

A) Post hoc identified PRF/GlyT2+ neurons (n=9 of 10 juxtacellularly recorded neuron)

B) Number of APs evoked at 1, 10, and 20 Hz during the stimulus trains in the same PRF/GlyT2+ neurons (50 ms window) normalized to the response to the first stimulus in the train (n=5 trains for each stimulus).



**Figure S3. The effect of spontaneous cortical activity on PRF/GlyT2+ neurons. Related to Figure 3.**

A) Scheme of the experiments ( $n=7$  mice) and a posthoc identified PRF/GlyT2+ ( $n=7$ , green) neuron filled with neurobiotin (red) and the overlapping (yellow) (bottom)

B) A representative example of a spontaneous state change under light ketamine-xylazine anesthesia together with the firing activity of a PRF/GlyT2+ cell.

Top: Wavelet transformation of the cortical LFP activity. Middle: Action potentials of a PRF/GlyT2+ cell, thick black lines correspond to the first action potential of the detected clusters. Blue line: synchronized and desynchronized states. Bottom: The raw LFP signal is shown in grey, and the amplitude variance of the LFP signal (moving SD in a sliding window) is in red. The black dashed line represents the variance threshold for synchronized and desynchronized periods. Periods labeled with X (gray shading) are transient states, excluded from the analysis (see Methods).

C) Autocorrelogram of a representative neuron during synchronized and desynchronized periods.

D) Mean cluster rate (number of clusters/LFP state length) during synchronized ( $n=348$ , mean: 1.32, SD: 0.57, median: 1.59) and desynchronized periods ( $n=270$ ). The two neurons shown in gray did not fire rhythmic AP clusters. ( $n=7$ , Wilcoxon Signed-Rank Test,  $p=0.032$ ) \*  $0.05 < p$ ; \*\*  $0.01 < p$ ; \*\*\*  $p < 0.001$ ; n.s. - no significant difference.

Source data are provided as a Source Data file. Scale bars: A)  $20 \mu\text{m}$ .

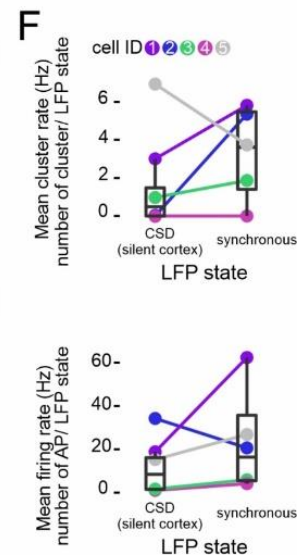
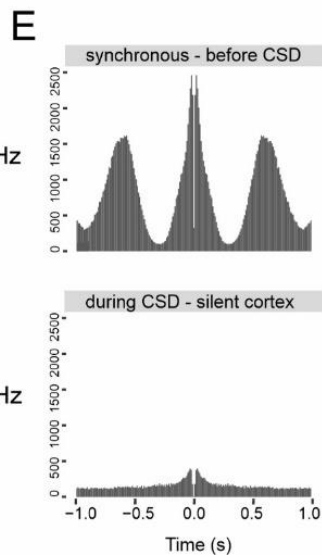
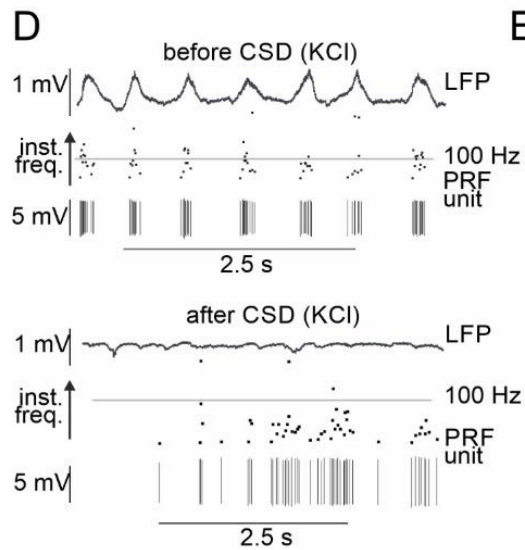
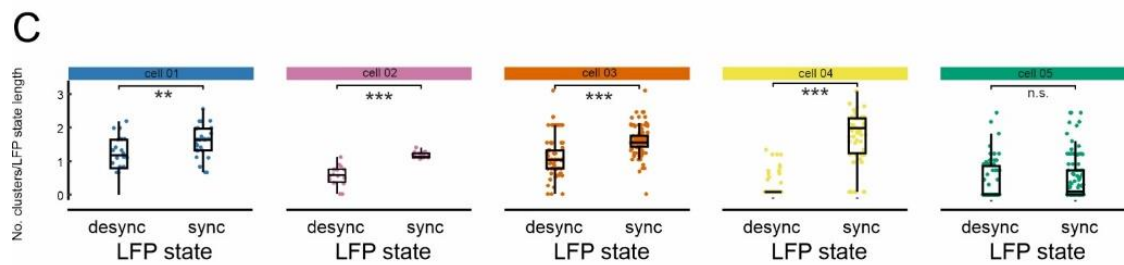
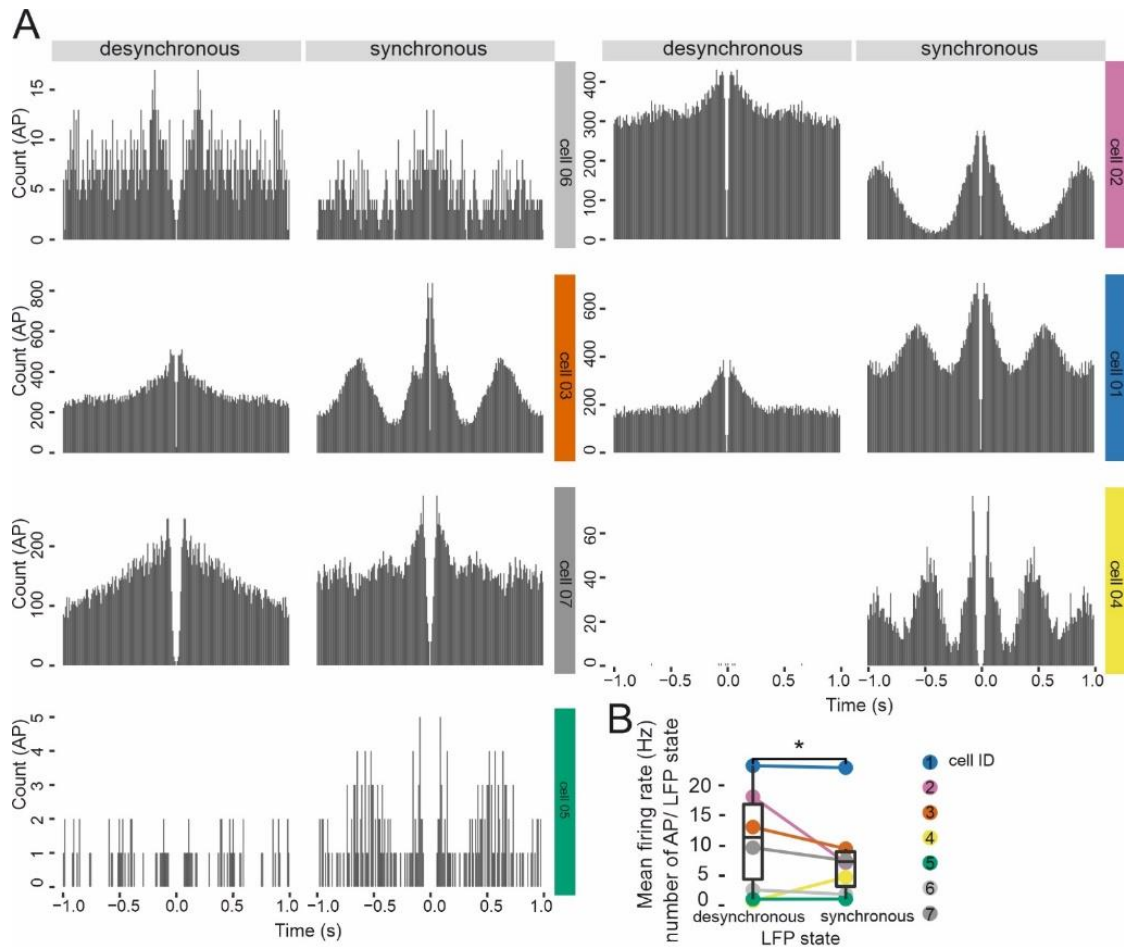


Figure S4. Autocorrelograms, mean cluster rate, and the effect of cortical spreading depression on PRF/GlyT2+ neurons. Related to Figure 3.

A) Autocorrelograms during synchronized and desynchronized LFP periods (n=7)

B) Mean firing rate (number of AP/LFP state length) during synchronized and desynchronized LFP periods. Wilcoxon Signed-Rank Test,  $p=0.031$ ,

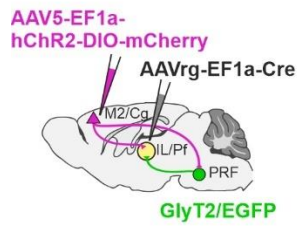
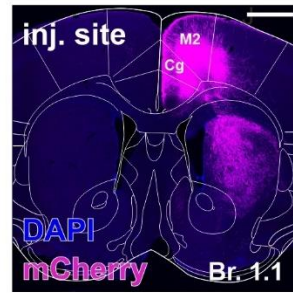
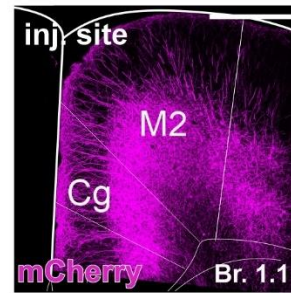
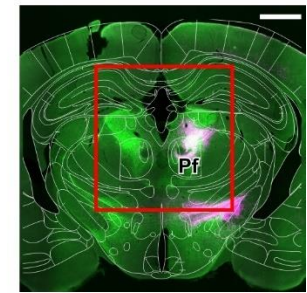
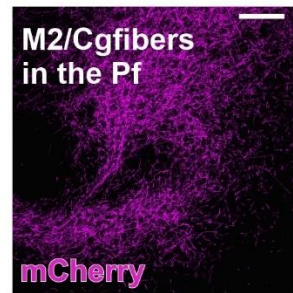
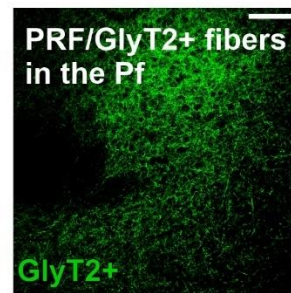
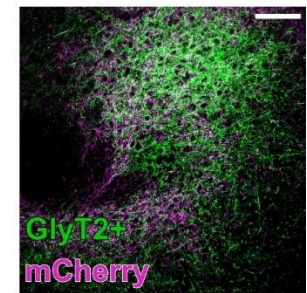
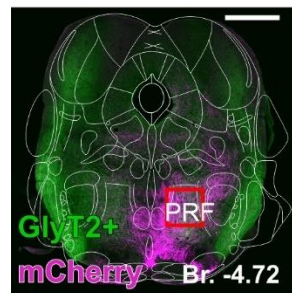
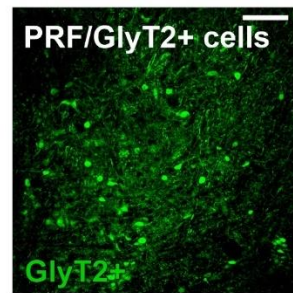
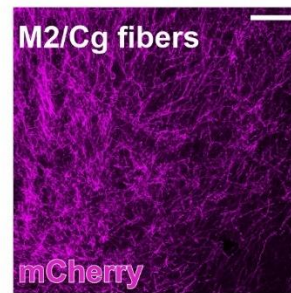
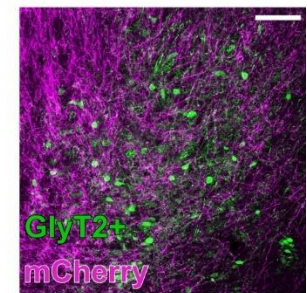
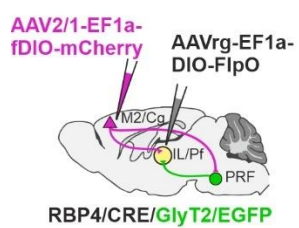
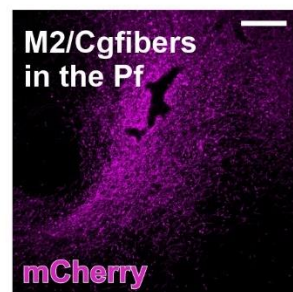
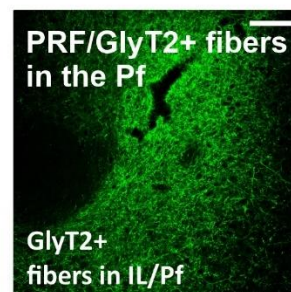
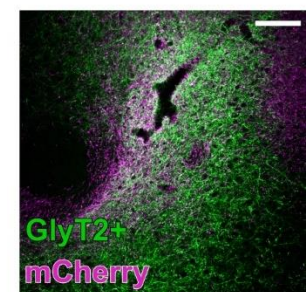
C) In four out of five cells, the mean number of clusters was significantly higher during synchronous vs desynchronous LFP states. Desynchronous vs. synchronous Mann-Whitney test; cell01  $p=0.0038$ ; cell02  $p<0.001$ ; cell03  $p<0.001$ ; cell04  $p<0.001$ ; cell05  $p=0.094$ , \*  $0.05<p$ ; \*\*  $0.01<p$ ; \*\*\*  $p<0.001$ ; n.s. - no significant difference. Source data are provided as a Source Data file.

D) Representative example of the baseline activity of a PRF neuron (top) and the changes in firing pattern following cortical inactivation using two molar KCl solution (cortical spreading depression, CSD) (bottom).

E) Autocorrelogram before CSD (top) and during CSD (bottom).

F) Mean cluster rate (number of clusters /LFP state length) during CSD (top) and mean firing rate (number of AP /LFP state length) during CSD (bottom) (n=5 neurons).

\*  $0.05<p$ ; \*\*  $0.01<p$ ; \*\*\*  $p<0.001$ ; n.s. - no significant difference. Source data are provided as a Source Data file

**A****B****C****D****E****F****G****H****I****J****K****L****M****N****O****P**

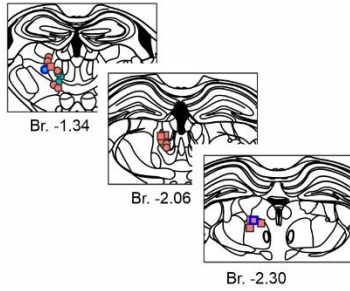
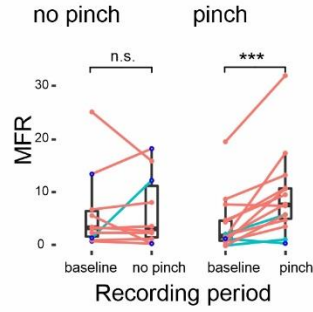
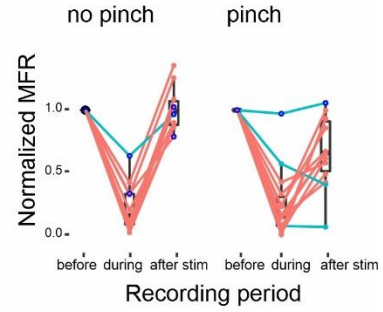
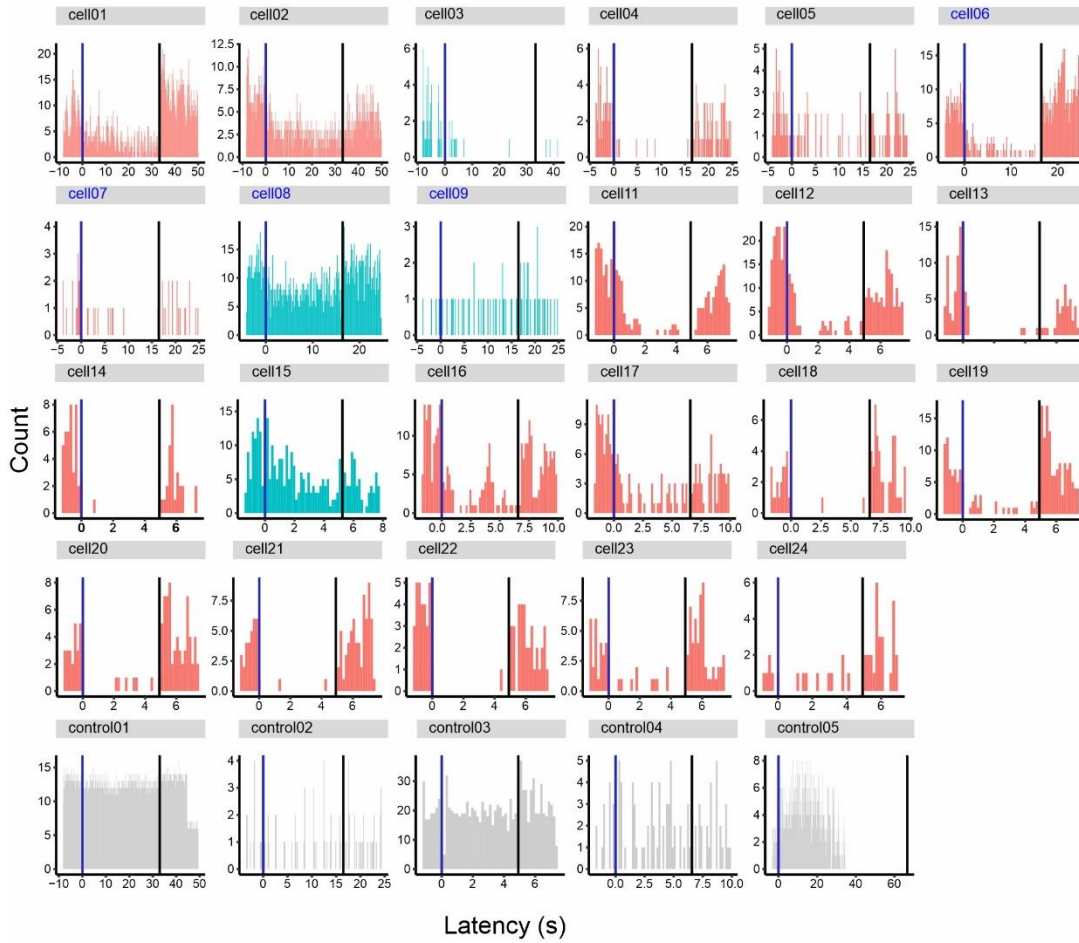
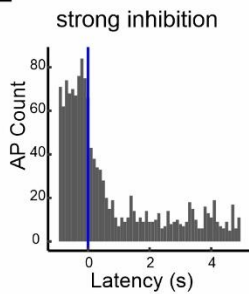
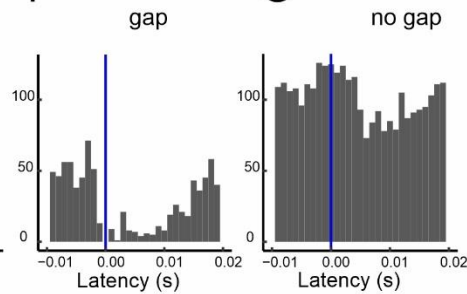
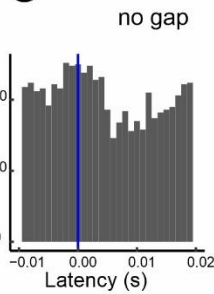
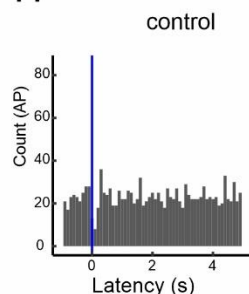
**Figure S5. Thalamus-projecting M2/Cg axon arbors in the PRF and the thalamus.  
Related to Figure 4.**

- A) Scheme of the second experimental design, double viral injection in GlyT2/eGFP mice  
B-C) Fluorescent micrograph of the cortical injection site, low power (B) and confocal image of the cortical neurons (C).  
D-E) Merged fluorescent image of the labeled thalamus-projecting M2/Cg cortical fibers (magenta) and PRF/GlyT2+ fibers (green) in the thalamus at lower (D) and higher (E) magnification. The red rectangle on D indicates the area in E and the red rectangle on E indicates the F-H position.  
F-H) Confocal image of the labeled thalamus-projecting M2/Cg cortical fibers (magenta, F), of the PRF/GlyT2+ fibers (green, G) and their merged image (H) in the thalamus.  
I) Composite fluorescent image of the labeled thalamus-projecting M2/Cg cortical fibers (magenta) and PRF/GlyT2+ fibers (green) in the brainstem  
J-L) Confocal micrographs of the PRF/GlyT2+ cells (green, J), anterogradely labeled thalamus-projecting M2/Cg cortical fibers (magenta, K), and their merged image (L)  
M) Scheme of the first experimental design (same as main Figure 5).  
N-P) Confocal image of the labeled thalamus-projecting M2/Cg cortical fibers (magenta, N), of the PRF/GlyT2+ fibers (green, O) and their merged image (P) in the thalamus in the first experimental design (M).  
Scale bars: B) 1 mm, C) 500  $\mu$ m, D-E) 1 mm, F-H) 100  $\mu$ m, I) 1 mm J-L) 100  $\mu$ m, N-P) 100  $\mu$ m.



**A**

□ no pinch ○ pinch ● gap

**B**Inhibitor strength  
● strong ● weak ● gap**C****D****E****F****G****H**

**Figure S6. Photostimulation-induced PRF/GlyT2+ mediated inhibition of IL/Pf thalamic neurons. Related to Figure 5.**

A) Position of the recorded IL/Pf neurons in the thalamus. Rectangles are neurons recorded with tail pinch; circles are neurons without tail pinch.

B) Comparison of mean firing rates of the IL/Pf neurons during the baseline vs before the stimulation. In the no pinch condition (n= 13 cell, left) the firing rate remains stable. In the pinch condition (right, n= 10 cell), neurons significantly increase their in response to a tail pinch. Strongly inhibited, (red circles, n=19 cell), weakly inhibited (light blue circles, n=4, see Methods) and neurons responding with a post-stimulus gap (dark blue circle, n=4) are indicated. No pinch (left) and pinch (right) conditions are shown separately. Wilcoxon Signed-Rank Test. Baseline vs. no pinch, n.s.; baseline vs. tail pinch,  $p < 0.001$ ,

C) Normalized mean firing rate (MFR) of a recorded IL thalamic neuron before, during, and after the photoactivation of PRF/GlyT2+ fibers. Labels as in B.

D) Individual PSTH of IL/Pf cell (strongly inhibited, red; weakly inhibited, blue) and non IL/Pf thalamic control neurons (grey) before during and after the photoactivation of PRF/GlyT2+ fibers. The stimulus duration was variable (5-30 sec). Gap neurons are indicated with blue cell number fonts.

E) Population PSTH of strongly inhibited IL/Pf neuron (n=19).

F) Population PSTH of IL/Pf neuron with a post-stimulus gap in activity (n=4) in the first 20 msec.

G) Short latency population PSTH of IL/Pf neuron without a gap (n=19).

H) Population PSTH of control neurons (n=5)

\*  $0.05 < p$ ; \*\*  $0.01 < p$ ; \*\*\*  $p < 0.001$ ; n.s. - no significant difference. Source data are provided as a Source Data file

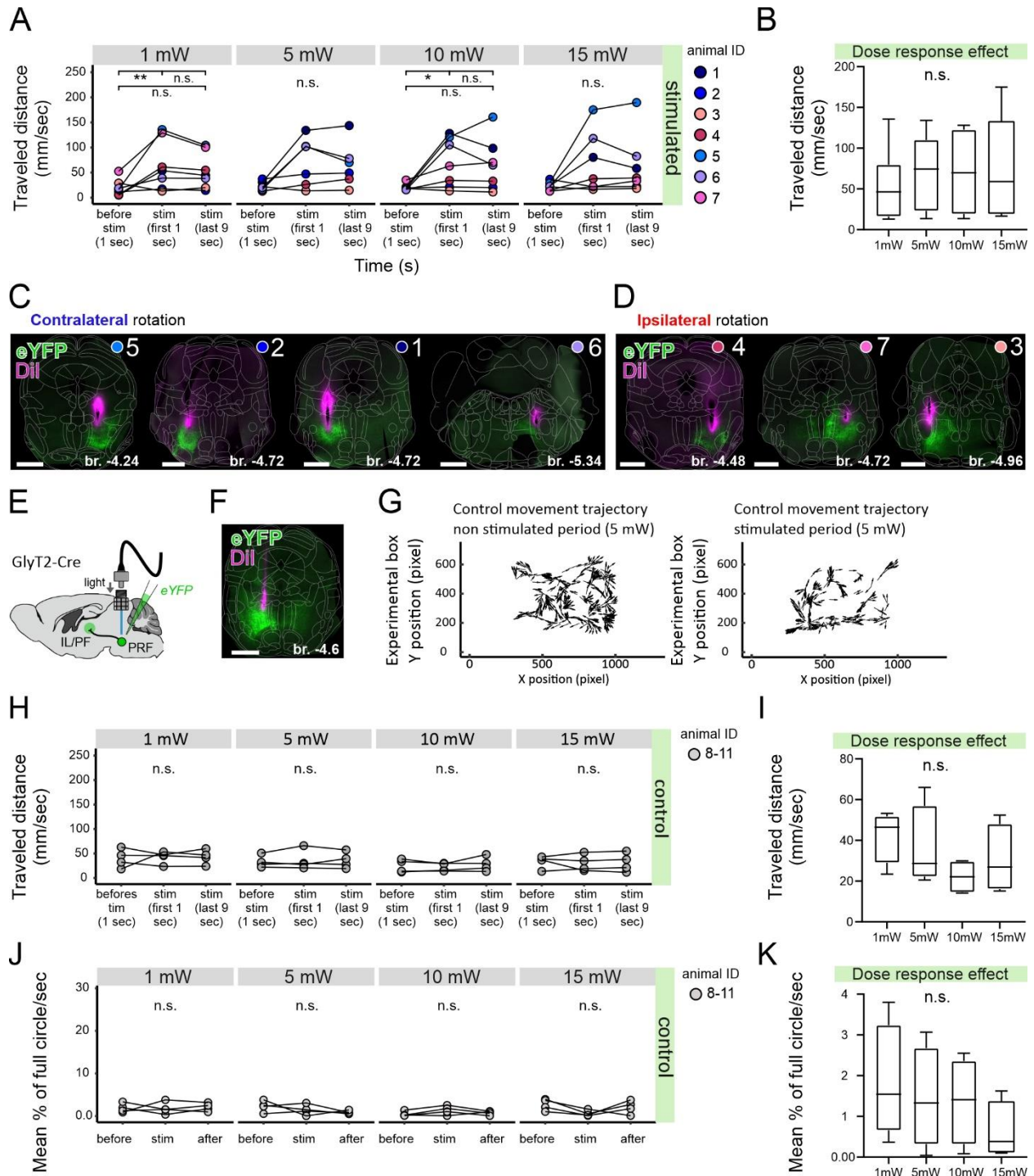
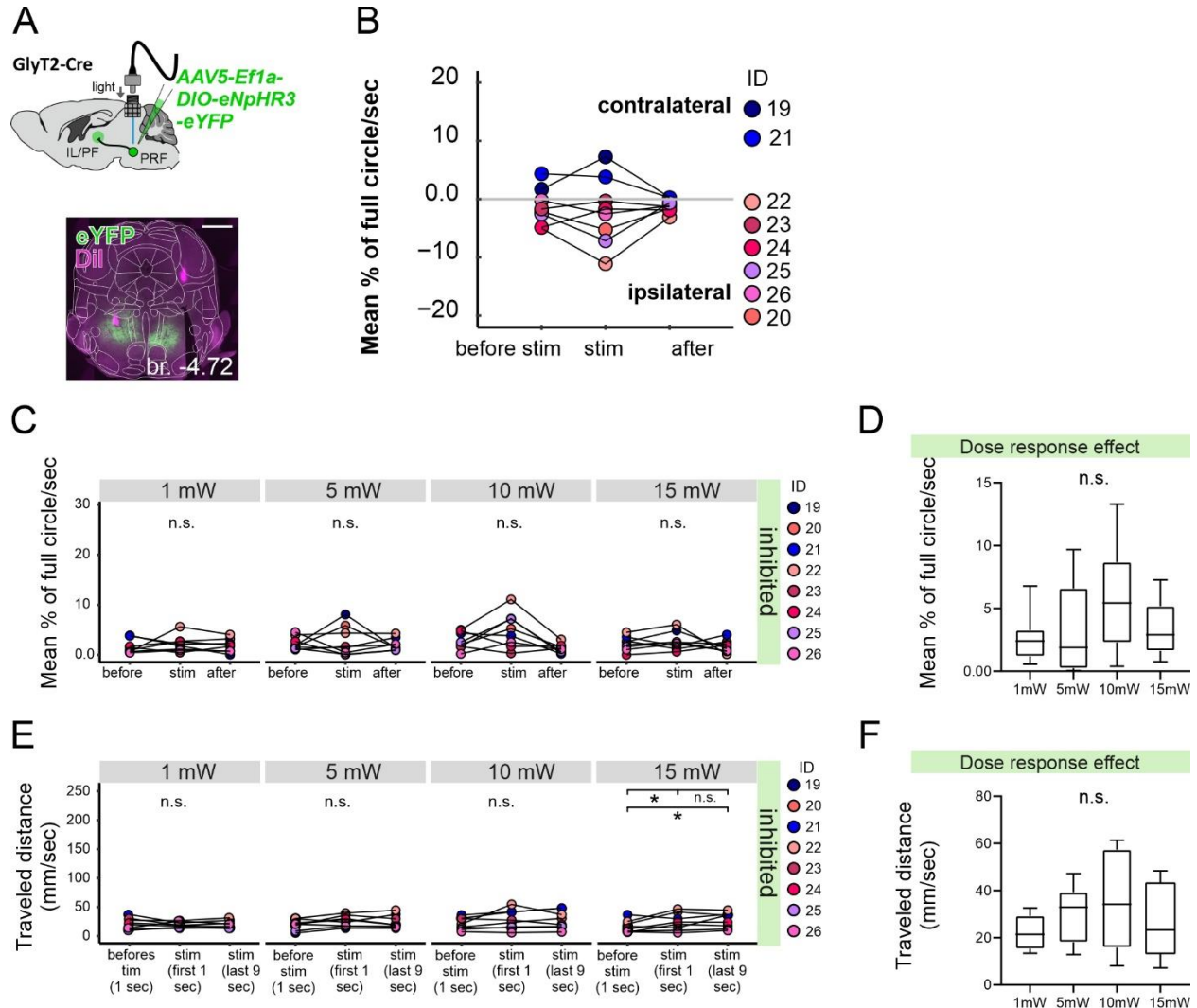


Figure S7. Behavioral effects of photoactivating PRF/GlyT2+ somata in experimental (ChR2) and control (EYFP) conditions. Related to Figure 6.

- A) Comparison of the traveled distance (mm/sec) before the stimulus, in the first 1 sec and the subsequent 9 sec during the stimulus in the experimental animals (n=7). Friedman test following Durbin-Conover post-hoc, 1mW  $\chi^2=7.14$ , p=0.028, before vs first 1 sec p=0.004, first 1 sec vs. last 9 sec n.s., before vs. last 9 sec n.s.; 5mW  $\chi^2=4.33$ , n.s.; 10mW  $\chi^2=9$ , p =0.050, before vs first 1 sec p=0.012, first 1 sec vs. last 9 sec n.s., before vs. last 9 sec n.s.; 15mW  $\chi^2=6$ , n.s., numbers indicate individual animals.
- B) Lack of dose-response effect at 1, 5, 10, and 15 mW laser power in experimental mice on movement initiation. Friedman test for first sec  $\chi^2=4.2$ , n.s.;
- C) Fluorescent micrographs of the implanted optic fibers in mice responding with contralateral rotation to unilateral activation of PRF/GlyT2+ somata. Numbers/color codes are the same as for A and Figure 7F, H, I.
- D) Fluorescent micrographs of the implanted optic fibers in mice responding with ipsilateral rotation to unilateral activation of PRF/GlyT2+ somata. Numbers/color codes are the same as for A and Figure 7F, H, I.
- E) Experimental design of the control behavioral experiments in GlyT2-Cre mouse.
- F) Fluorescent micrographs of the implanted optic fiber in representative control mice.
- G) Movement trajectory in one representative control mouse during the non-stimulated period (left) and the stimulated period (right) at 5 mW.
- H) Comparison of the traveled distance (mm/sec) before the stimulus, in the first 1 sec and the subsequent 9 sec during the stimulus in control animals. Friedman test 1mW  $\chi^2=1.5$ , n.s.; 5mW  $\chi^2=0.5$ , n.s.; 10mW  $\chi^2=0$ , n.s.; 15mW  $\chi^2=0.5$ , n.s.;
- I) Lack of dose-response effect at 1, 5, 10, and 15 mW laser power in control mice on movement initiation. Friedman test for first sec  $\chi^2=6.9$ , n.s.;
- J) Control animals' mean rotation angle before, during, and after stim periods. Friedman test 1mW  $\chi^2=0$ , n.s.; 5mW  $\chi^2=1.5$ , n.s.; 10mW  $\chi^2=1.5$ , n.s.; 15mW  $\chi^2=4.5$ , n.s
- K) Lack of dose-response effect at 1, 5, 10, and 15 mW laser power in control mice on rotation. Friedman test for first sec  $\chi^2=1.2$ , n.s.
- \* 0.05<p; \*\* 0.01<p; \*\*\* p<0.001; n.s. - no significant difference. Source data are provided as a Source Data file.
- Scale bar: C-D) 1 mm F) 1 mm



**Figure S8. Behavioral effects of photoinhibiting PRF/GlyT2+ somata. Related to Figure 6.**

**A)** Top: Experimental design of the photoinhibition behavioral experiments in GlyT2-Cre mouse Bottom: Fluorescent microscopic post hoc identification of implanted optic fiber and virus injection site (green) in one representative photoinhibited mouse. The appropriate optic fiber position was on the left side of the PRF labeled with Dil (magenta).

**B)** Separation of the absolute rotational values into contralateral and ipsilateral rotations. The data is displayed as the mean rotation angle before, during, and after the stimulus periods following PRF/GlyT2+ soma inhibition at all intensities.

**C)** Mean rotation angle of photoinhibited animals before, during, and after stim periods. Friedman test 1mW  $\chi^2=3$ , n.s.; 5mW  $\chi^2=0.25$ , n.s; 10mW  $\chi^2=3.25$ , n.s.; 15mW  $\chi^2=1$ , n.s

**D)** Lack of significant dose-response effect on rotation at 1, 5, 10, and 15 mW in control mice Friedman test for first sec  $\chi^2=4.2$ , n.s.

**E)** Comparison of the traveled distance (mm/sec) before the stimulus, in the first 1 sec and the subsequent 9 sec during the stimulus in photoinhibited animals. Friedman test following Durbin-Conover post-hoc 1mW  $\chi^2=2.25$ , n.s.; 5mW  $\chi^2=5.25$ , n.s.; 10mW  $\chi^2=1.75$ , n.s.; 15mW  $\chi^2=7.75$ , p=0.021, before vs first 1 sec p=0.039, first 1 sec vs. last 9 sec n.s., before vs. last 9 sec p=0.003

**F)** Lack of significant dose-response effect on movement initiation at 1, 5, 10, and 15 mW in control mice. Friedman test for first sec  $\chi^2=3.45$ , n.s.;

\* 0.05<p; \*\* 0.01<p; \*\*\* p<0.001; n.s. - no significant difference. Source data are provided as a Source Data file.

Scale bar: A) 1 mm

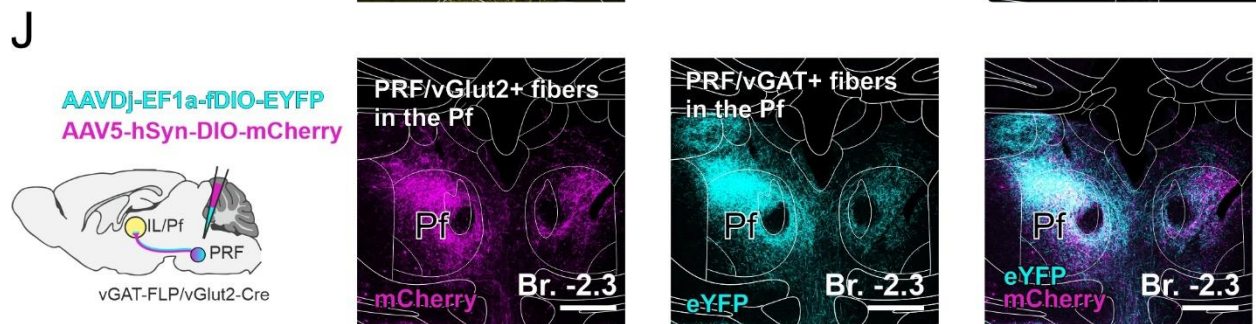
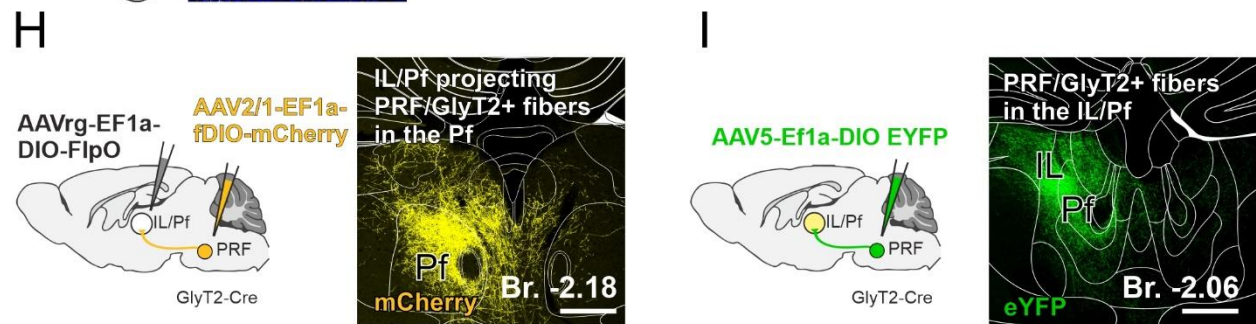
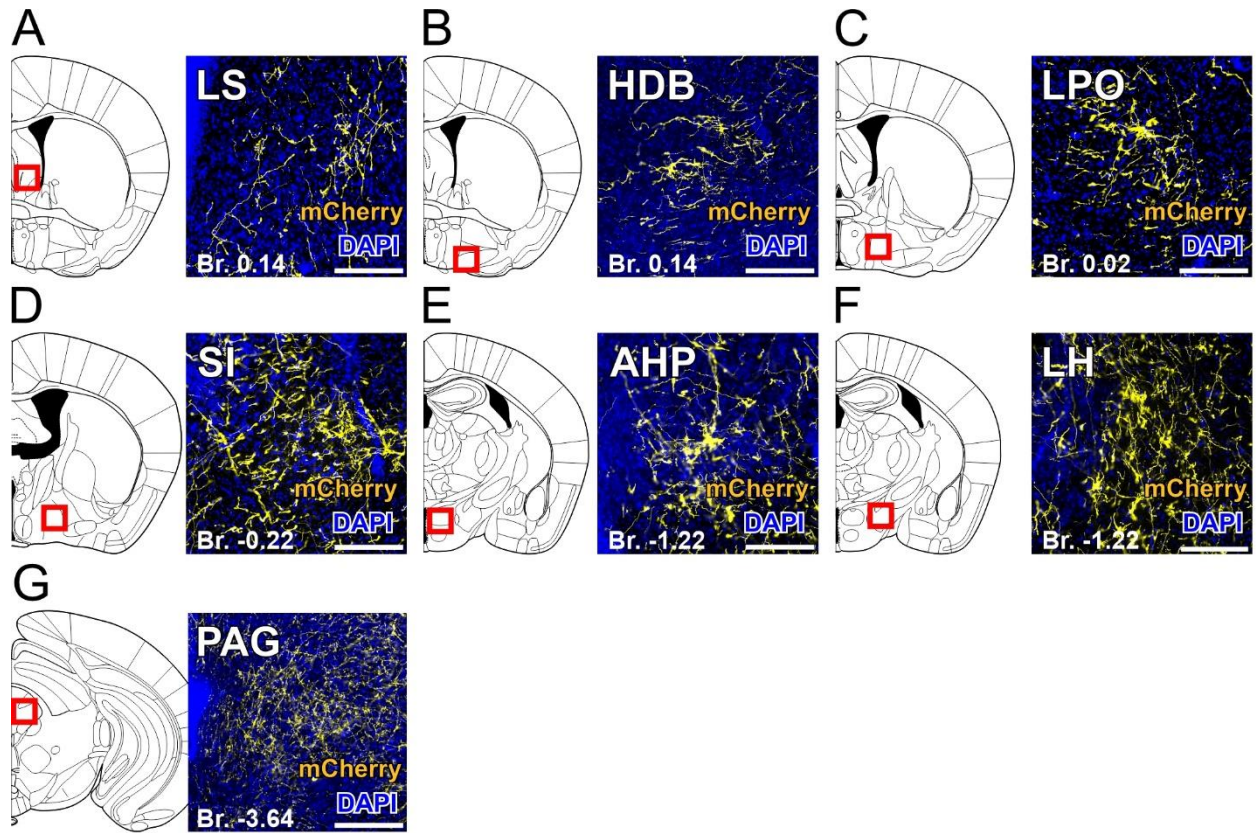


Figure S9. Efferents of thalamus-projecting PRF/GlyT2+. Related to Figure 7.

- A) Thalamus-projecting PRF/GlyT2+ axons in the lateral septum (LS).
  - B) Thalamus-projecting PRF/GlyT2+ axons in the nucleus of the horizontal limb of the diagonal band (HDB).
  - C) Thalamus-projecting PRF/GlyT2+ axons in the lateral preoptic area (LPO).
  - D) Thalamus-projecting PRF/GlyT2+ axons in the substantia innominate (SI).
  - E) Thalamus-projecting PRF/GlyT2+ axons in the anterior hypothalamus (AHP).
  - F) Thalamus-projecting PRF/GlyT2+ axons in the lateral hypothalamus (LH).
  - G) Thalamus-projecting PRF/GlyT2+ axons in the periaqueductal grey (PAG).
  - H) Scheme of double conditioned viral tracing for investigating the thalamus-projecting PRF/GlyT2+ cells' efferents in GlyT2-Cre mice (right) and their axons in the thalamus (left).
  - I) Experimental design to label all PRF/GlyT2+ cells (left) and their axons in the thalamus (right).
  - J) Scheme of mixed viral injection into PRF in vGAT-Flp/vGlut2-Cre (right) and their vGlut2+ fibers (magenta); PRF/vGAT+ fibers (cyan) and merged confocal image of the vGlut2+ and vGAT+ fibers (left) in the Pf.
- Scale bars: A-G) 200  $\mu$ m, H-J) 500  $\mu$ m.



## Supplemental tables

Table S1. Co-innervation of PRF,IL/Pf and the striatum by single L5 neurons. Related to Figure 4.

Co-innervation of PRF and IL/Pf by single L5 neurons					
DOI	Soma's position	Entire name	PRF axonal endpoint	IL/Pf axonal endpoint	striatal axonal endpoint
AA0179	MOs5	Secondary motor area layer 5	1	2	+
AA0845	ACAv5	Anterior cingulate area ventral part layer 5	1	0	-
AA0115	MOs5	Secondary motor area layer 5	2	4	+
AA0764	ACAd5	Anterior cingulate area dorsal part layer 5	2	3	+
AA0796	ACAv5	Anterior cingulate area ventral part layer 5	3	0	-
AA0882	MOs5	Secondary motor area layer 5	3	0	-
AA1544	MOs5	Secondary motor area layer 5	3	4	-
AA0181	MOs5	Secondary motor area layer 5	4	44	+
AA0415	MOs5	Secondary motor area layer 5	4	2	+
AA0576	MOs5	Secondary motor area layer 5	4	1	+
AA0792	MOs5	Secondary motor area layer 5	4	20	+
AA0182	MOs5	Secondary motor area layer 5	5	14	+
AA0250	MOs5	Secondary motor area layer 5	6	1	+
AA0780	MOs5	Secondary motor area layer 5	6	7	+
AA1538	MOs5	Secondary motor area layer 5	6	0	-
AA0114	MOs5	Secondary motor area layer 5	7	5	+
AA0791	MOs5	Secondary motor area layer 5	8	6	+
AA0180	MOs5	Secondary motor area layer 5	9	0	-
AA1541	MOs5	Secondary motor area layer 5	12	0	-
AA0772	MOs5	Secondary motor area layer 5	19	31	+
AA0788	MOs5	Secondary motor area layer 5	19	6	+
AA0261	MOs5	Secondary motor area layer 5	37	36	+
AA0245	MOs5	Secondary motor area layer 5	39	34	+

Neuron database based on Janelia Mouse Browser. DOI: Janelia ID for neurons. Soma's position name was determined by Janelia's nomenclature PRF and IL/Pf axonal endpoint means how many afferents the PRF has from M2/Cg. In the striatal axonal endpoint column, the +/- indicates whether there was M2/Cg's afferent.